OPTIMAL SYNTHESIS OF AN ELASTIC SUSPENSION SYSTEM FOR A MARINE REDUCTION GEAR BY MULTIBODY MODELLING

Matteo Codda
CETENA S.p.A.
via Ippolito D'Aste 5 – 16121 Genova – Italy
matteo.codda@cetena.it

Pietro Fanghella
DIMEC – Univ. of Genoa
via Opera Pia 15ᵃ – 16145 Genova – Italy
pietro.fanghella@unige.it

Raffaele Iaccarino
CETENA S.p.A.
via Ippolito D'Aste 5 – 16121 Genova – Italy
raffaele.iaccarino@cetena.it

Abstract. *This paper describes how a multibody model of a marine reduction gear can be used to investigate the design of unconventional supporting solutions. Marine reduction gears are traditionally rigidly connected to the ship hull but, when noise transmission has to be drastically reduced, elastic mounting may be required. The dynamic behaviour of a complete reduction gear is represented by a multibody model containing compliant representations of bearings, shafts and gear meshes. Once such a model has been validated, a supporting system is introduced: the position and stiffness of elastic supports are parameterized and then made dependent on few design variables. The optimisation routine provided by the multibody code determines the optimal values of the above mentioned design variables, according to the objective function: its formulation tends to minimize the natural frequencies of the reduction gear, considered as a rigid body supported by the suspension system. The interaction with other elements of the propulsion line is taken into account in the design problem by means of constraints on the optimisation formulation: excessive misalignments of the reduction gear with the shaft line are prevented by limiting the loads on certain bearings, whereas misalignments with the gas turbines are directly constrained, on the basis of the functional requirements for the relevant coupling joints. This paper proves how a simulation tool can be effectively used to make a feasibility study of a complex problem of industrial interest. Moreover, the virtual model can be adjusted according to different design specifications and levels of generality.*

Keywords: *elastic suspension, resilient mounting, marine reduction gear, multibody dynamics, optimisation.*

1. Introduction

The reduction of noise and vibrations is becoming a crucial challenge to be faced in ship design. Both passenger and naval vessels have to satisfy more and more demanding noise and vibration requirements, due to different reasons: enhancement of onboard comfort for ferries and cruise ships and minimization of acoustic signature for military ships.

In these highly technological ships, there are many sources of noise and vibrations, such as propellers, auxiliary plants, generators, but one of the most important is the propulsion system; when the prime mover is a high-speed engine (gas turbine, diesel engine), the typical configuration of the plant is: prime mover – coupling joint – gearbox – shaft line – propeller.

Of the two major excitation sources, represented by the mover and the gearbox, only the first is usually elastically suspended and isolated from the ship hull: gear and gearbox manufacturers state that, even with hard mounted arrangements, low noise requirements can normally be met thanks to high-quality machining techniques.

On the other hand, it is commonly agreed that, when noise transmission has to be drastically reduced, elastic mounting may be required (Luz and Boyle, 1998, Willhelm, 2002): depending on acceptable noise levels, complexity of the overall system and costs, either metallic or elastomeric mounts may constitute the best design option. This is because the more compliant elastomeric mounts guarantee the lowest transmission of noise at the cost of the highest motion of the gearbox; therefore, more complex couplings with the prime mover and, possibly, a high torque coupling joint with the shaft line may be required. The latter is definitely a very complex and expensive component, which can be made redundant by use of stiffer metallic mounts: these ensure worse noise-transmission performances but lower motion of the gearbox.

The goal of the present study is the development of a simulation model to synthesize a suspension system for a large-sized marine reduction gear.

The general assumption on which the whole study is based is that the level of performance of the considered suspension system, from the point of view of noise transmission, is inversely related to the stiffness of the suspensions, i.e., it is assumed that a softer suspension has a better behaviour than a stiffer suspension (Smith, 1999).

The simulation model will take into account the limitations imposed by the functional requirements for the gearbox interfaces, and will calculate the optimal characteristics of the suspension system in terms of position and stiffness of the supports; the actual design and engineering of such supports are beyond the scope of the present work and will not be considered.

The model of the propulsion system discussed in the following section is based on a real design, which has been simplified and adapted when necessary, especially as regards aspects considered secondary for the purpose described.

2. Description of the system

The propulsion line, as shown in the schematic of Fig. 1, includes two gas turbines (GT), connected to the two input shafts of the gearbox by two coupling joints (CJ); the single output shaft of the gearbox is rigidly connected to the shaft line by a flange. The shaft line, at whose end a variable pitch propeller is placed, is supported by 10 bearings (B_1 … B_{10}) and one thrust bearing (TB), which carries both longitudinal and lateral loads.

In nominal conditions, each gas turbine supplies 22 MW at 3600 rpm, whereas the low-speed shaft rotates at about 140 rpm; the length of this shaft, from the propeller to the flange with the gearbox, is approximately 110 m .
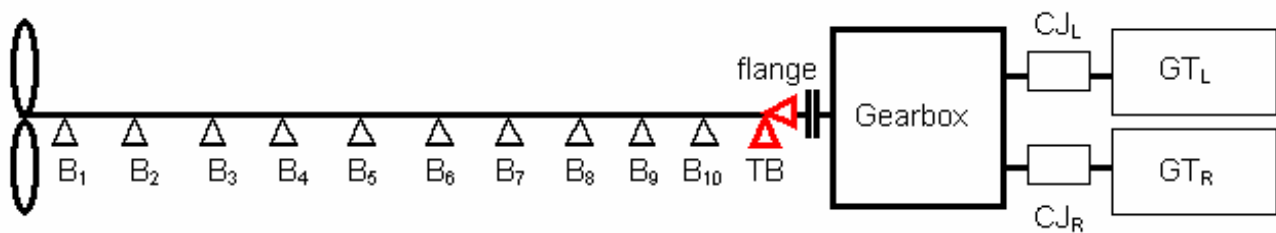
Figure 1. Schematic of the propulsion system.

A 3D view of the rotating parts of the gearbox is presented in Fig. 2, whereas a projected view is visible in Fig. 3. The torque coming from the two gas turbines is transmitted to the two input shafts through the coupling joints (right CJ_R, left CJ_L); the input shafts are connected to the high speed pinions (right HSP_R, left HSP_L) via two self-synchronizing clutches (right Cl_R , left Cl_L); here the torque path is split, with each high-speed pinion engaging two first reduction gears (upper-right $1RG_{UR}$, lower-right $1RG_{LR}$, upper-left $1RG_{UL}$, lower-left $1RG_{LL}$).
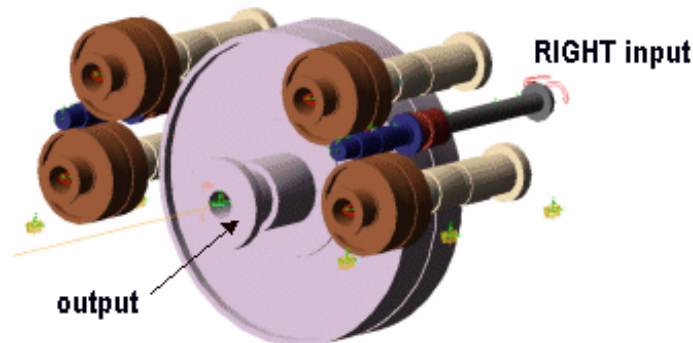
Figure 2. 3D view of the gearbox rotating parts.

The first reduction gears are connected to the low-speed pinions (upper-right LSP_{UR} , lower-right LSP_{LR} , upper-left LSP_{UL} , lower-left LSP_{LL}) by flexible quill shafts; finally, the four low-speed pinions engage the second reduction gear, which is rigidly connected to the shaft line by a flange.

The rotating shafts are supported by 26 hydrodynamic bearings (gB_1, gB_2, … gB_{26}), arranged as shown in Fig. 3.

Both first and second reduction meshes are configured in a double-helical arrangement.
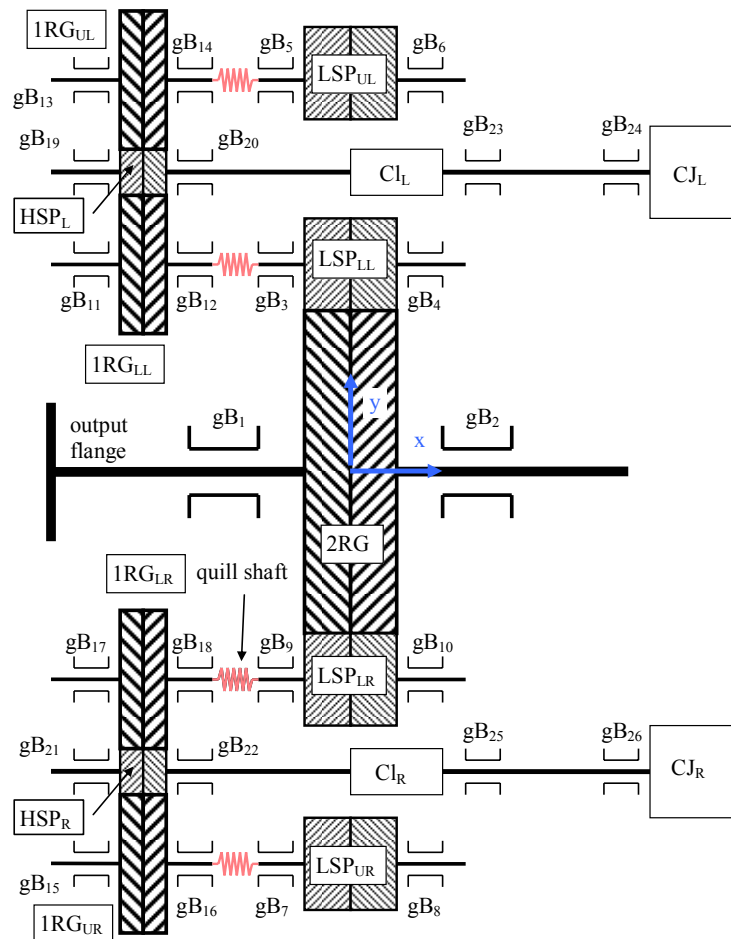
Figure 3. Projected view of the gearbox rotating parts.

3. Simulation model of the propulsion system

A multibody approach has been selected as the primary simulation tool; in particular, a multibody model of the propulsion system, starting from the coupling joints between the gearbox and the gas turbines up to the propeller, has been set up. The gas turbines themselves have not been included, as uncoupled by the coupling joints from the rest of the plant and therefore not influencing the synthesis of the suspension system.

A mobility analysis of the system, schematised in Fig. 1 and Fig. 3, reveals the possibility of incurring a large number of redundant constraints: every shaft is supported by several bearings; for each input pinion, there are two in-parallel shafts connecting it to the output wheel 2RG; the shaft line is supported by 11 bearings.

As outlined in Section 6, the design of the suspension system will take into account limitations on the values of reaction forces in some critical bearings; therefore, a proper computation of the forces in the system is required in order to carry out the optimisation process. Such a result could not be achieved through a model containing redundant constraints, so they have been eliminated via the systematic replacement of kinematic and rigid components with compliant elements: all bearings and gears in the reducer have been represented by viscous-elastic components, whereas the shaft line has been modelled by a flexible body.

The final model used for the synthesis of the suspension system contains several rigid bodies, one flexible body, elastic couplings, and compliant models of all hydrodynamic bearings in the speed reducer. The evaluation of stiffness and damping data for such couplings and bearings has been one of the major difficulties with the present project. Several sources have been employed: in some cases, technical data were available for specific components; in other cases, ad hoc models were used for stiffness computation; finally, data from the scientific literature (Derek 1999, Rivin 1999) have been used. Nevertheless, there still is a significant uncertainty on physical parameters, especially regarding damping values. The complexity of this problem is partially overcome by the adopted synthesis procedure, which is mainly based on the study of the system in steady-state conditions (full power).

Unless otherwise stated, a global reference frame has been be used, with the origin in the second reduction gear centre, the x-axis along the shaft line (from aft to bow), the z-axis vertical and the y-axis transversal, pointing portside.

3.1. Rigid bodies

The rigid bodies making up the multibody model are: the *ground*, which is the still inertial reference body, two *input shafts*, including the two clutches (not modelled) and the two high-speed pinions, four *first reduction gears*, four *low-*

speed pinions, the *second reduction gear&shaft* and the *case*. A fixed kinematic joint has been defined between the second reduction gear and the shaft line: it represents the connecting flange.

All these bodies have been modelled in a CAD system and then imported into the multibody environment with inertial properties automatically calculated; the teeth geometry has not been included, as the gear contact forces have been modelled as described in Section 3.6.

3.2. Intermediate quill shafts

The four quill shafts connect first reduction gears to low-speed pinions and, together with them, form the four intermediate assemblies; they are the most flexible elements of the kinematic chain, hence their flexibility has been taken into account. As shown in Fig. 4, the two gears are connected by an intermediate link (magenta shape in Fig. 4) whose elastic behaviour is represented in the multibody model by a beam force element and whose mass has been equally distributed to the attached first reduction gears (light blue) and low-speed pinions (cyan). Section properties of the beam element have been defined according to the geometric properties of the component (circular section).
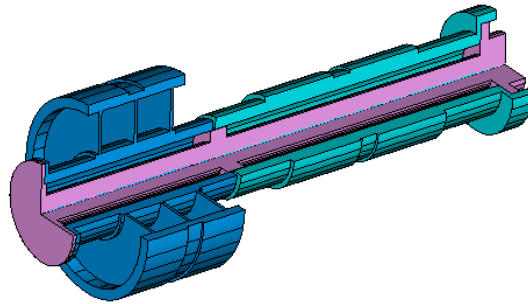
Figure 4. 3D representation of the quill shaft.

3.3. Coupling joints

The main function of the coupling joints connecting the gearbox and the gas turbines is to uncouple the motion of the turbines, usually elastically suspended, and to allow small translational and angular misalignments between the two subsystems.

The behaviour of these joints can be schematised by a system of three consecutive linear springs: one axial spring, with stiffness K_{ax}, and two bending springs, with stiffness K_{bend}. In order to simulate these components through bushing elements, the resulting stiffness characteristics, in global directions, have been calculated as follows:

$$K_x = K_{ax} = 8.82 \cdot 10^5 \, \frac{N}{m} \qquad K_y = K_z = \frac{K_{bend}}{2 \cdot L^2} = 1554 \, \frac{N}{m} \qquad K_{rotY} = K_{rotZ} = \frac{K_{bend}}{2} = 19421 \, \frac{Nm}{rad}$$

where L is the length of the component.

3.4. Gearbox bearings

All gearbox bearings have been modelled by linear bushing elements; for the sake of simplicity and considering that the detailed dynamic behaviour of the bearing themselves is beyond the scope of this paper, gearbox bearings have been divided into three classes: high-speed, intermediate-speed and low-speed bearings. For each class, the coefficients for radial stiffness and damping have been specified for the considered working conditions.

For all classes, the order of magnitude of the stiffness is 10^9 N/m, while, as far as the damping is concerned, its order of magnitude is 10^7 Ns/m (high-speed) and 10^8 Ns/m (intermediate and low-speed).

3.5. Shaft line

The small displacements of the gearbox case allowed by the suspension system must be compensated for by some form of compliance on the output side of the speed reducer. The classical solution based on the use of a coupling joint cannot be adopted due to the very high torque to be transmitted. Therefore, both in the real system and in the model, case displacements must be absorbed by the shaft line and the bearing flexibility. More specifically, in the model, the shaft line bearings have been assumed to be infinitely stiff and have therefore been modelled by kinematic constraints preventing lateral displacements of the shaft. The assumption is justified by the fact that, due to the long distance from the gearbox, the small displacements allowed by these bearings do not play a key role in the design of the suspension system.

On the contrary, the shaft line is modelled by a flexible body: the flexibility of this part cannot be neglected, because it has to bear the most significant portion of the relative motion and misalignment of the gearbox with respect to the ship hull.

According to the usual procedure for importing flexible bodies into multibody environments, an FE model of the shaft line, from the propeller to the flange with the gearbox, has been developed and validated. A particular beam element, able to include all rotational inertial properties, has been used for the mesh, which is characterized by an average element length of 0.25 m. The propeller has been represented by an equivalent hollow cylinder, whose inner and outer radii lead to the required mass and rotational inertia (including the contribution of the entrained water).

The generation of the modal basis used to represent shaft flexibility has followed the Craig-Bampton approach: attachment nodes have been defined at the two ends of the line (propeller and flange) and at the center of each bearing. This, together with the choice of the frequency range of interest, has resulted in a total modal basis of 90 mode shapes for the flexible body. Such a relatively high figure is due more to the large number of attachment nodes than to the frequency range of interest. As a matter of fact, the elastic behaviour of the shaft line, which plays an essential role in the analyses performed, is a quasi-static one, since only the steady state of the propulsion system has been studied.

3.6. Teeth contact model

A global approach to the modelling of the contact forces among teeth has been chosen: instead of representing the actual contact force between each pair of mating teeth, only the resultant of these has been calculated and applied to the ideal contact point of the pitch circumferences. With reference to Fig. 5 and considering the two angular variables for the pinion (θ_1) and for the gear (θ_2), with a common positive reference direction (according the right-hand rule), a Cartesian reference frame can be defined with its origin placed at the intersection of the two pitch circumferences, its x-axis pointing from the centre of the pinion to the centre of the gear, and the z-axis parallel to the positive direction of the angular positions.
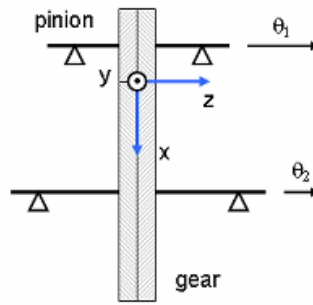
Figure 5. Contact force model: sign conventions and reference frame.

Defining:

$$E_\theta = \vartheta_1 + \tau\vartheta_2 \qquad\qquad \text{position transmission error}$$
$$E_\omega = \dot{\vartheta}_1 + \tau\dot{\vartheta}_2 = \omega_1 + \tau\omega_2 \qquad\qquad \text{velocity transmission error}$$

where τ is the reduction ratio of the gear mesh, the torsional moment of the gear on the pinion can be written as:

$$M_{GP} = -K \cdot E_\theta - D \cdot E_\omega$$

where K and D are the stiffness and damping coefficients of the gear mesh.

The resultant force of the gear on the pinion can therefore be expressed as:

$$F_{GPx} = -\frac{|M_{GP}|}{R_P}\tan(\alpha) \qquad\qquad F_{GPy} = -\frac{M_{GP}}{R_P}$$

and the opposite force of the pinion on the gear as:

$$F_{PGx} = \frac{|M_{GP}|}{R_P}\tan(\alpha) \qquad\qquad F_{PGy} = \frac{M_{GP}}{R_P}$$

where α is the transversal pressure angle and R_P is the pitch radius of the pinion; no axial force is defined, due to the double helical arrangement of the gear mesh.

One of the characteristics of this viscous-elastic model is that, in steady-state conditions, the nominal torque can be transmitted only if a certain angular position error occurs: this results from the fact that the pinion and gear teeth bend under load.

4. FE models for mesh stiffness evaluation

The mesh stiffness coefficient described in Section 3.6. has been evaluated, for both the first and second reduction stages, by a numerical procedure based on FE modelling.

Assuming that the torsional stiffness of the gear mesh is governed only by the bending stiffness of the teeth in contact, FE plain strain models of the pinion and gear teeth have been developed; a master node has been defined in the centres of the pinion and of the gear and, for each of the two bodies, all nodes at the teeth roots have been rigidly connected to them (see Fig. 6).
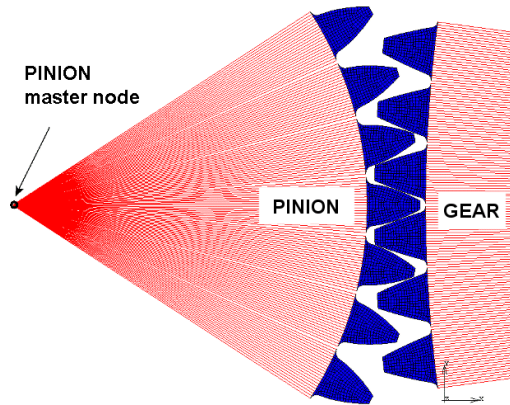
Figure 6. Pinion and gear master nodes.
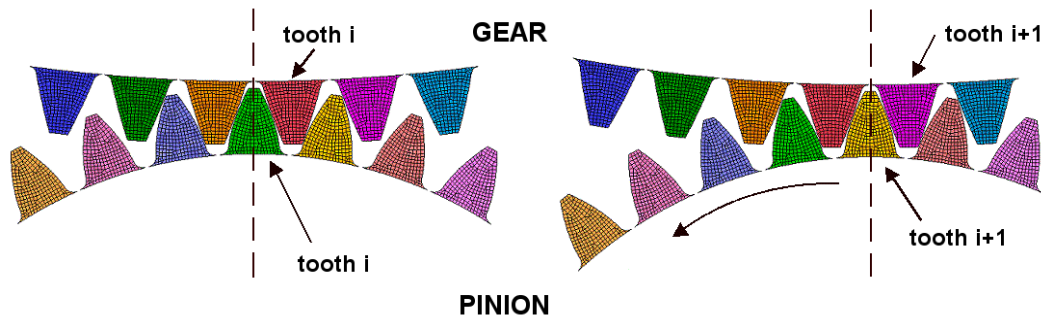
Figure 7. FE model: first and last configuration.

Having defined a contact relation between the mating teeth of the pinion and the gear, and keeping the gear master node fully constrained, incremental rotations have been imposed on the pinion master node: the applied moment vs. angular rotation relationship has been evaluated, by non-linear static analyses. The same procedure has then been repeated for 10 consecutive configurations of the gear mesh, until the $i+1^{th}$ tooth has taken the place of ith (see Fig. 7).

A typical moment (per unit length) vs. rotation curve is shown in Fig. 8; the multi-linear shape is the consequence of varying contact conditions. Every time a new node of the pinion touches one tooth of the gear, the slope increases; it is foreseeable that the curve would get smoother with finer meshes.

The stiffness coefficient, for a configuration, is the slope of the curve at a torque value corresponding to the nominal level; the total stiffness has been calculated as the average of the 10 configurations analysed (Tab. 1).

Table 1. Stiffness coefficients for the two reduction stages.

	1st reduction	2nd reduction
Stiffness (Nm/rad)	$3.96 \cdot 10^8$	$2.07 \cdot 10^9$

It is worth noting that, even if fully 3D FE models of double helical gear meshes could have been dealt with by modern hardware and software, these simple 2D models require a very short computational time and only a small additional post-processing of the results.
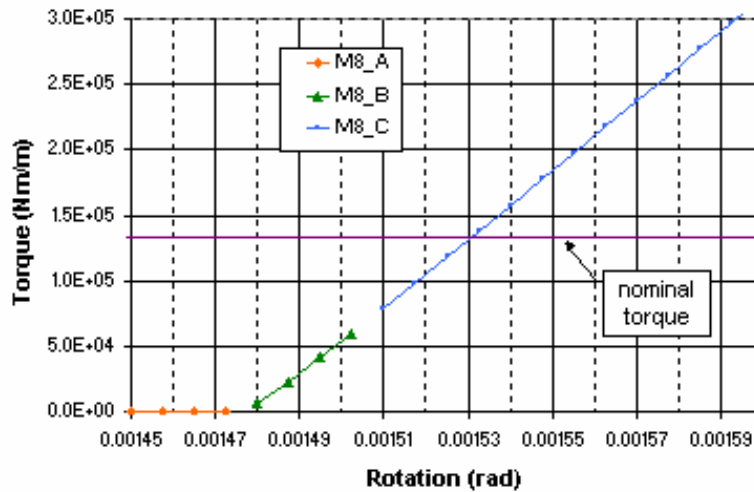
Figure 8. Typical torque vs rotation curve.

5. Reference model: hard-mounted gearbox

In order to validate the model and to establish a baseline for the subsequent optimisation process, a hard-mounted configuration of the gearbox has been analysed: full-power, steady-state conditions have been chosen in which both gas turbines provide 22 MW at 3600 rpm. The action of the turbines is modelled by two constant torque elements, defined at the fore ends of the input shafts.

The reaction of the propeller is also represented by a torque defined at the aft end of the output shaft; this assumption does not affect the dynamic behaviour of the gearbox but simplifies the model since the flexible shaft line does not bear any torsion. Similarly, no propeller thrust has been defined, as it would have been carried by the thrust bearing. The relation adopted for the propeller torque, according to the cubic law relating the power supply of the propulsion plant to the ship speed, is the following:

$$T = P_{max} \cdot \frac{\omega^2}{\omega_{max}^3}$$

where T is the propeller reaction torque, ω is the propeller angular velocity, P_{max} is the maximum power of the propulsion plant, and ω_{max} is the nominal angular velocity at the maximum power.

Angular-velocity initial conditions have been defined for the input shafts, intermediate shafts and low-speed shaft, with the aim of reducing the initial transient conditions and of reaching steady-state conditions as quickly as possible. From the time histories of some output variables shown in Fig. 9, it can be realised how the system stabilizes approximately in 1 second. The following 2 seconds of simulation time are used to get steady-state values of all variables involved in the optimisation process.
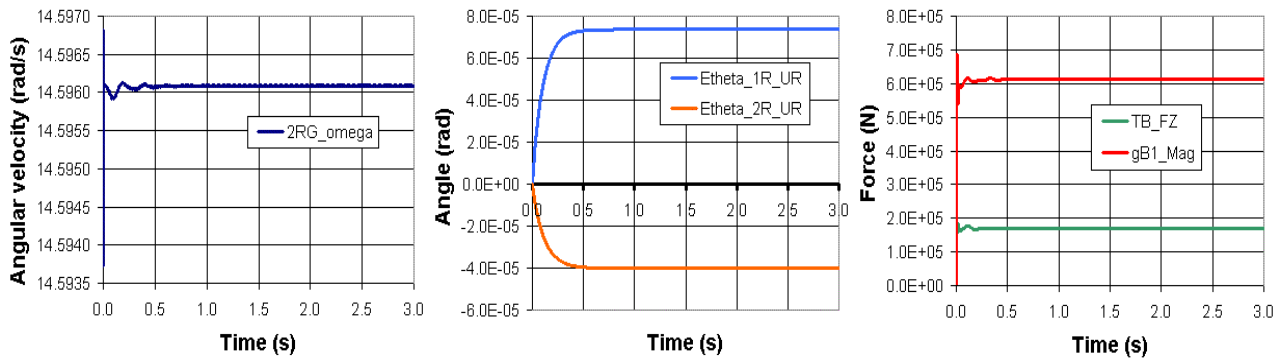
Figure 9. Hard mounted configuration – (a) angular velocity of the 2nd reduction gear, (b) position transmission errors of the upper right 1st and 2nd-stages, (c) magnitude of the gB1 load and vertical reaction of the thrust bearing.

6. Synthesis of the suspension system

Based on the real design proposed by Bryant, 1985, a suspension system has been introduced into the model; it is composed by eight equal isolators, six of which have been placed vertically and two longitudinally (Fig. 10); the vertical isolators have been named A_i and the longitudinal isolators B_i.
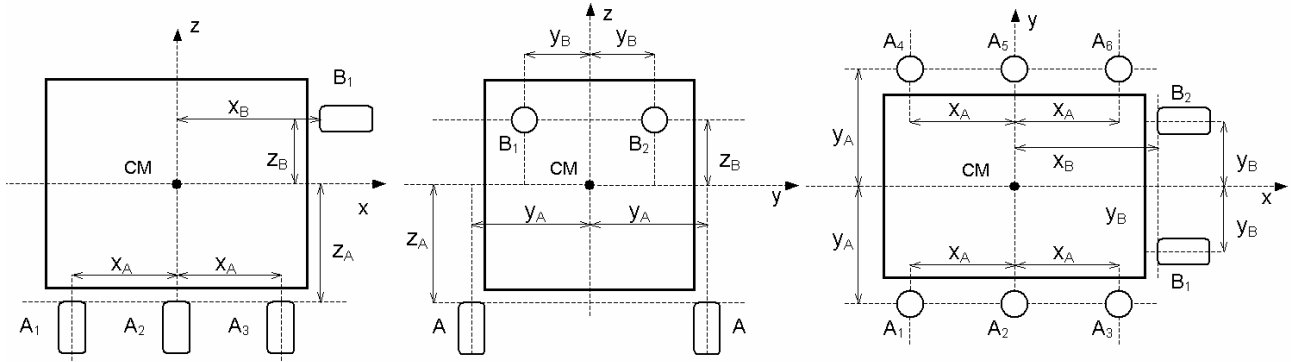
Figure 10. Positions of the isolators.

The layout adopted for the suspension system has many degrees of symmetry: the vertical isolators (group A) are symmetrical with respect to the *yz* and *zx* planes of a reference frame located in the gearbox centre of mass (CM); moreover, they are placed on one common horizontal plane ($z = z_A$). The longitudinal isolators are symmetrical with respect to the *xz* plane and are placed on common transversal ($x = x_B$) and horizontal ($z = z_B$) planes. It can be easily noticed how the whole layout of the suspension system may be driven by means of only six parameters, namely, x_A, y_A, z_A, x_B, y_B, z_B, whose definitions can be derived from Fig. 10.

One of the assumptions made about the isolators is their cylindrical symmetry: hence, the elastic suspensions have been modelled by bushing elements, defined between the bodies *ground* and *case*, which have been completely characterized by two stiffness (K_a – axial, K_r – radial) and two damping (D_a – axial, D_r – radial) coefficients.

As already pointed out in Section 1, an efficient and then adequately soft suspension system inevitably allows misalignments of the gearbox with respect to the other components of the propulsion line. This may lead to bad contact conditions of the gear teeth and to a consequent reduction in the gearbox efficiency and working life. As a matter of fact, a suspension system must decrease noise and vibrations transmission without compromising the good performance of the gearbox. For this reason, the optimisation problem implemented includes constraints representing the functional requirements of the gearbox and its interfaces, i.e., the coupling joints and the fore part of the shaft line. In particular, requirements for the coupling joints have been figured out by the relevant data sheet, in terms of maximum allowable translational and angular misalignments between their extremities $\left(\delta_x, \delta_y, \delta_z, \theta_y, \theta_z\right)$, while, for the shaft line, limits on the bearing reaction forces have been set.

In marine propulsion shaft alignment, the load on bearings is the common indicator of acceptable working conditions, has to be equally distributed among similar bearings and, where a gearbox is present, must be well balanced between the bull gear bearings. Major deviations from the design load usually imply unsafe working conditions for the bearings and, possibly, bad teeth contact conditions. Considering the shaft line arrangement in its foremost part, as shown in Fig. 11, constraints on the optimisation procedure have been imposed, limiting the overloads of the vertical reactions of the thrust bearing (R_{TBz}) and of the two bearings of the second reduction gear (R_{GB1} and R_{GB2}), with respect to the reference design values $\left(\widetilde{R}_{TBx}, \widetilde{R}_{GB1}, \widetilde{R}_{GB2}\right)$.
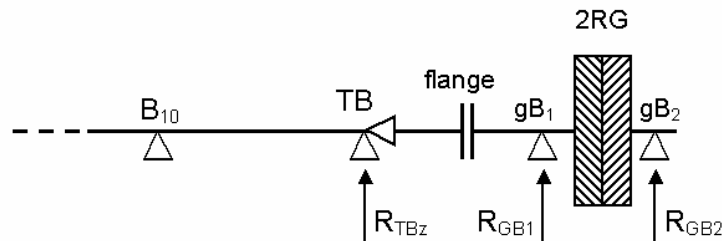
Figure 11. Shaft line arrangement: foremost part.

Finally, assuming that the noise and vibrations transmission of the elastic suspension system is inversely related to its stiffness, an objective function has been defined that tends to minimize the maximum natural frequency of the gearbox, considered as an isolated body suspended on the elastic mounts. From the layout of the isolators, shown in Fig. 10, the six total stiffness coefficients (3 translational and 3 rotational around CM) of the suspension system may be calculated as a function of the 8 design parameters, as follows:

$$K_{totX} = 6K_r + 2K_a \qquad\qquad K_{totY} = 8K_r \qquad\qquad K_{totZ} = 6K_a + 2K_r$$

$$K_{totRX} = 6y_A^2 K_a + 2\cdot\left(3z_A^2 + y_B^2 + z_B^2\right)\cdot K_r \qquad\qquad\qquad (1)$$

$$K_{totRY} = 2\cdot\left(2x_A^2 + z_B^2\right)\cdot K_a + 2\cdot\left(3z_A^2 + x_B^2\right)\cdot K_r \qquad\qquad K_{totRZ} = 2y_B^2 K_a + 2\cdot\left(2x_A^2 + 3y_A^2 + x_B^2\right)\cdot K_r$$

The six uncoupled natural frequencies of the gearbox have then been evaluated by the following approximate expressions, in which M, J_{xx}, J_{yy} and J_{zz} are the mass and diagonal terms of the inertia matrix of the complete speed reducer:

$$f_X = \frac{1}{2\pi}\sqrt{\frac{K_{totX}}{M}} \qquad\qquad f_Y = \frac{1}{2\pi}\sqrt{\frac{K_{totY}}{M}} \qquad\qquad f_Z = \frac{1}{2\pi}\sqrt{\frac{K_{totZ}}{M}}$$

$$f_{RX} = \frac{1}{2\pi}\sqrt{\frac{K_{totRX}}{J_{XX}}} \qquad\qquad f_{RY} = \frac{1}{2\pi}\sqrt{\frac{K_{totRY}}{J_{YY}}} \qquad\qquad f_{RZ} = \frac{1}{2\pi}\sqrt{\frac{K_{totRZ}}{J_{ZZ}}}$$

The comprehensive definition of the optimisation problem is summarized in Tab. 2:

Table 2. Summary of the optimisation routine

Design variables	$x_A\ y_A\ z_A$	locations of isolators – group A
	$x_B\ y_B\ z_B$	locations of isolators – group B
	K_a	axial stiffness of isolators
	K_r	radial stiffness of isolators
Constraints	$1.4m \le x_A \le 2m$ $1.5m \le y_A \le 2.7m$ $-1.2m \le z_A \le 1m$	ranges of design variables driving the locations of group A isolators
	$1m \le x_B \le 1.5m$ $0.5m \le y_B \le 0.9m$ $0.5m \le z_B \le 1.3m$	ranges of design variables driving the locations of group B isolators
	$10^7\ N/m \le K_a \le 10^{10}\ N/m$ $10^5\ N/m \le K_r \le 10^9\ N/m$	ranges of design variables driving axial and radial stiffnesses of isolators
	$-20.2mm \le \delta_x \le 8.83mm$ $\left\|\delta_y\right\| \le 24mm$ $\left\|\delta_z\right\| \le 24mm$	maximum translational misalignments allowed by coupling joints
	$\left\|\theta_y\right\| \le 0.55°$ $\left\|\theta_z\right\| \le 0.55°$	maximum angular misalignments allowed by coupling joints
	$85\%\widetilde{R}_{TBz} \le R_{TBz} \le 115\%\widetilde{R}_{TBz}$	maximum deviation of the vertical thrust bearing load from reference values
	$85\%\widetilde{R}_{GB1} \le R_{GB1} \le 115\%\widetilde{R}_{GB1}$	maximum deviation of first bull gear bearing load from reference
	$85\%\widetilde{R}_{GB2} \le R_{GB2} \le 115\%\widetilde{R}_{GB2}$	maximum deviation of second bull gear bearing load from reference values
Objective function	$\min\left(\max\left(f_X, f_Y, f_Z, f_{RX}, f_{RY} f_{RZ}\right)\right)$	minimization of the highest natural frequency of the gearbox

The results of the optimisation routine are graphically shown in Fig. 11 and numerically given in Tab. 3. It can be observed how the objective function is governed by the rotational natural frequency f_{RX} around x-axis (Fig. 12 (a)) and how all the other frequencies decrease in much the same manner. The lowest value of the objective function is actually reached during the second iteration but the solution is discarded because of the violation of some constraints; in optimal conditions, the constraint on the vertical reaction load of the thrust bearing is active.

The highest changes in the design variables occur for the axial (-53%) and radial (-75%) stiffnesses of the isolators (Fig. 12 (b)); the influence of the optimisation process on the location design variables is less significant and the major

changes occur in y_A (-15%, see (Fig. 12 (c))), which plays the main role in the expression of the governing natural frequency (Eq. (1)).

Table 3. Tabular output of the optimisation: design variables and objective function

Iteration.	K_a (N/m)	K_r (N/m)	X_A (m)	X_B (m)	Y_A (m)	Y_B (m)	Z_A (m)	Z_B (m)	f_{RX} (Hz)
0	1.00E+08	1.00E+07	1.7	1.3	2.1108	0.84115	0.7	0.7	147.8
5	4.65E+07	2.65E+06	1.774	1.3032	1.81	0.85037	0.6805	0.73587	86.2
variation	-53.5%	-73.5%	4.4%	0.2%	-14.3%	1.1%	-2.8%	5.1%	-41.7%
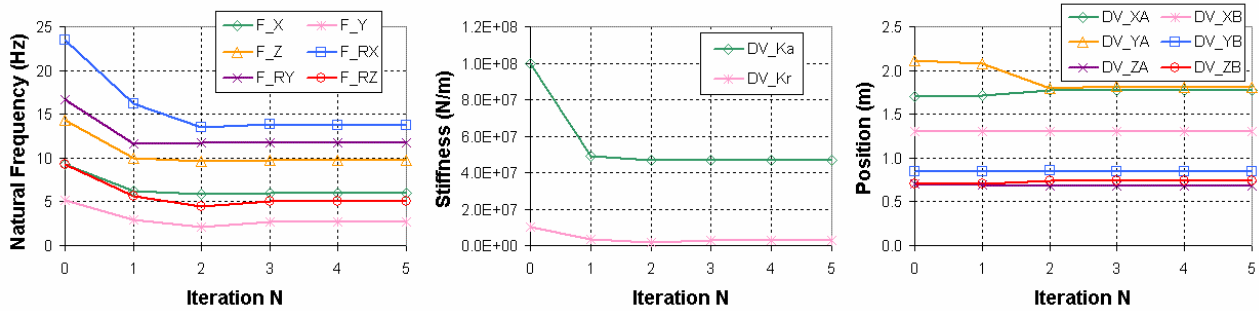
Figure 12. Optimisation results – (a) natural frequencies, (b) isolators' axial and radial stiffnesses, (c) location design variables of groups A and B vs. iteration number.

7. Conclusions

This paper has illustrated how a simulation model can be used to make a feasibility study investigating innovative or unconventional design alternatives; in particular, the elastic mounting of a large-sized marine reduction gear has been studied through a multibody model of the propulsion system. Mathematical representations of several components and phenomena have been presented and discussed: then they have been applied by an optimisation routine to synthesize the optimal arrangement of the suspension system. It is important to stress that, once the model has been set up, element attributes, constraints and the objective function can be easily adjusted to meet various design requirements.

The model described, which is an example of effective integration and synergy among different software families (solid modellers, FE solvers, multibody analysers), allows higher levels of generality and complexity. Other working conditions, like transients or split plant configurations, could be considered, together with more exhaustive behaviours of certain components, such as the flexibilities of the gearbox case and of the shafts.

8. Acknowledgements

9. References

Bryant, R., 1985, "The Development of the DDG-51 High Power Density Gear", Proceedings of SNAME Spring Meeting/STAR Symposium, Norfolk, VA., May 21-24, 1985, pp 25-37.

Luz, J. J. and Boyle, D. A., 1998, "Low Noise Mechanical Drive Propulsion System Alternatives", Proceedings of ASNE Symposium 21st Century Combatant Technology, 27-30 January 1998, Biloxi, MS, USA.

Rivin, I. E., 1999, "Stiffness and Damping in Mechanical Design", Marcell Dekker, ISBN 0-8247-1722-8

Smith, J. D., 1999, "Gear Noise and Vibration", Marcell Dekker, ISBN 0-8247-6005-0.

Vicari A., 2003, "Elastic Mounting of a Marine Reduction Gear: Feasibility Study by Multibody Modelling", Ms Thesis, University of Genoa - DIMEC (in Italian).

Willhelm, S., 2002, "Resilient Gearbox Mounting: Efficient Noise Control for Royal Clipper", The Naval Architect, January 2002, pp. 10-11.

10. Responsibility notice

The authors are the only responsible for the printed material included in this paper.